# Architectural Decisions for Communications Satellite Constellations to Maintain Profitability While Serving Uncovered and Underserved Communities

Inigo del Portillo*, Sydney I. Dolan, Bruce G. Cameron, Edward F. Crawley

*Department of Aeronautics and Astronautics, 77 Massachusetts Avenue, Cambridge, 02139, USA*

**Abstract**

The rise of the commercial space industry has resulted in the development of mega-constellations that promise to provide global broadband. These constellations capitalize on advancements in technology, improved modeling capabilities, and reductions in launch cost. One of the significant open questions is whether these constellations will significantly increase access for uncovered and underserved communities, in addition to serving existing markets. This paper analyzes which constellation characteristics provide the best global coverage at the lowest operational cost. First, we present the demand model that assesses the number of under-served and uncovered users in a given region. Then, we present a genetic algorithm used to identify potential constellations. Finally, we conclude by identifying which characteristics are the most promising for broadband constellations, as well as predictions of how the market will develop in the coming years. Our analysis has found that geostationary (GEO) and medium Earth orbit (MEO) satellite constellations have the highest likelihood of profitability. LEO networks are on average 27% more expensive, but if designed wisely, they can be competitive. Our work shows that there are diminishing returns with large constellations, and that it is more cost effective to have a small number of highly capable satellites, rather than many low complexity satellites. Key technologies like high frequency bands and miniaturization of components can lead to further cost reductions and increase the competitiveness of LEO constellations.

*Keywords:* communication satellites, low Earth orbit constellation, mega-constellation, space internet, global broadband

## 1. Introduction

### *1.1. Motivation*

The concept of using constellations to provide global broadband was first proposed during the 1990s. Unfortunately, many of those systems failed due to poor market evaluation and long lead times to operation [1]. Demand modeling failed to account for additional drivers to adoption, like service quality and the handset attributes, and by the time the satellites were operational, the

*Corresponding author

*Email address:* inigo.del.portillo@gmail.com (I. del Portillo),sydneyd@mit.edu (S. I. Dolan), bcameron@mit.edu (B. G. Cameron),crawley@mit.edu (E. F. Crawley), (Edward F. Crawley)

market had shifted considerably [2]. In recent years, demand forecasting has only become more complicated with the development of additional technologies like voice calling over the internet, the development of new services like video streaming which are very intensive in data consumption, and the widespread use of mobile telephones. These services affect the forecasting price accuracy, market competitiveness, and settlement rate (i.e., the price paid by the originating company to the receiving company to connect international calls) predictions [3].

The newly proposed constellations are different from their predecessors from the 90s in two main aspects: first, the democratization and increasing demand for connectivity services worldwide, and second, the advancements in technology, manufacturing, and launch systems, which result in lower costs and allow for the deployment systems of a much larger scale (ranging from tens of satellites to thousands). These constellations vary in design and configuration, operating at different altitudes, inclinations, and with a different number of orbital planes. SpaceX has filed documents for an initial 4000-satellite constellation in Low Earth Orbit [4]. In contrast, other commercial providers like OneWeb have an estimated constellation size of 648 satellites[5], whereas ViaSat plans to operate a MEO constellation of 20 satellites [6]. It remains to be seen which constellation architectures are profitable, or if larger constellations result in a system that is overcapacity.

This paper analyzes how different constellation designs compare, and we assess which constellations could be used to provide basic connectivity to uncovered and under-served region in developing countries. In contrast to prior work in this field that focused on the area covered, this paper incorporates global broadband demand modeling by utilizing econometric models of uncovered and under-served users.

This paper evaluates the characteristics of communications architectures and the potential impact of these systems to connect additional populations that have no connectivity or only 2G connectivity.The International Telecommunication Union Resolution 200 – Connect 2020 Agenda for Global Telecommunication[7] and the UN Broadband [8] listed connecting the world's population to the internet as one of their top priorities. While the first billion individuals connected to the internet had a monthly disposable income of $82.04 for communication services, the same measure for the last billion is $0.90 [9]. Although the number of internet users is increasing, Philbeck predicted that some continents have almost reached a saturation with more than 80% of the population connected [10], they will have to effectively cover underserved markets that have less capital available while maintaining a profit to operate and provide communications services. Prior work in the field has studied a few constellation configurations and their coverage, but this paper develops a comprehensive approach across a range of orbits (LEO, GEO, and MEO) and design variable (inclinations, number of satellites, and orbital planes), which will be adjusted to identify the most cost-effective configurations to extend connectivity to uncovered and under-served regions. The scope of this paper does not include latency-sensitive services for which a comparison across LEO, MEO, and GEO would not represent a fair comparison.

To that end, a comprehensive model to calculate both the cost to operate the system and the sellable capacity (i.e., performance) is developed. In addition, the model analyzes the economic viability of each design configuration. These result complement existing studies on quantifying the demand from uncovered users, by providing an estimate on the available market of users that could utilize broadband internet but have yet to. To address the concern of affordability and to have a high-fidelity estimate of the demand, the cost of living and relative pricing for various regions across the world is incorporated into the model.

### 1.2. Paper objective and contributions

The main objective of this paper is to compare the quality of different constellation designs in providing broadband connectivity to uncovered and underserved populations. To that end, we propose a method to systematically enumerate constellation designs based on a small set of decisions, search the space of potential architectures looking for the best points, and analyze what decisions have the most impact on the performance and cost of the architectures.

In doing so, this paper presents the following contributions:

- A new model to evaluate the performance and cost of large constellations of satellite to provide global communications.
- A tradespace exploration study comparing the sellable throughput and capital-expenditure (CAPEX) cost of different constellation designs, including six currently proposed constellations.
- A study on the potential impact of satellite-constellations in bringing uncovered and underserved populations online.

### 1.3. Paper structure

The paper is structured as follows. Section 2 presents the literature review in terms of constellation modeling, constellation design optimization, and demand estimation. Section 3 introduces the methodology and models used in the analysis, whereas Section 4 validates these models against historical data. Section 5 presents the results of the tradespace exploration of constellation designs, and Section 6 summarizes the conclusions of the analysis.

## 2. Literature Review

### 2.1. Constellation Modeling and Design Optimization

Prior work has studied the technical viability of proposed commercial architectures, such as Telesat, OneWeb, and SpaceX [11]. This study evaluated the system throughput, satellite efficiency, and required ground station infrastructure for each constellation, and revealed that modern commercial companies diverge in their technical strategy. OneWeb focused on being first-to-market with minimal risk and complexity, whereas Telesat focused on capability and flexibility at the cost of added complexity, and SpaceX opted for a large-scale design, which brings associated complexity and risk. The differences in strategy highlight the uncertainty surrounding optimal constellation design for broadband coverage.

In addition, existing work in the field has evaluated broadband coverage using constellations in orbits ranging from GEO [12] [13] to LEO [14], highlighting the benefits and drawbacks of each orbit. LEO possesses a more benign radiation environment, which enables the use of more commercial off-the-shelf (COTS) components [12]. MEO constellation require less satellites, which means lower capital expenditure (CAPEX) and lower service costs. Comparing this historically, the high CAPEX and service costs were part of the reason for the limited commercial success of Iridium and Globalstar[15]. With carefully phased arrays and advanced technologies in higher frequency bands, highly inclined GEO satellites could be a technically and commercially feasible and attractive solution for mobile satellites [12]. Similarly, prior work has evaluated the impact of inter-satellite links (ISL's) on the satellite coverage, and speculated that they could reduce the number

of required ground stations [12]. GEO, MEO, and LEO satellites with free space optical links can be a commercially viable backbone, if physical topology, link capacity and routing strategy are be carefully addressed [16] as well as the technical viability [17].

Due to the computational complexity associated with determining the optimal constellation configurations, early methods focused on comparing the benefits of a subset of characteristics such as orbital altitude, inclination, and number of satellites, by simplifying some of the characteristics through a Walker Constellations[18][19] . Walker Constellations possess symmetric geometry, which makes them suitable for global coverage [20], and are configured so that the orbital parameters are dependent on one another to reduce complexity.

Adaptive genetic algorithms have been shown to reduce simulation time for constellation modeling, aiding in improved ability to identify optimal architectures with better coverage maps [21]. Crossley and Williams studied simulated annealing and genetic algorithm approaches for coverage of a latitude region. Their work revealed that both methods found constellation designs that outperform the classical Walker design at low Earth central angles [22]. More recently, work in constellation modelling has shifted to utilizing multi-objective genetic algorithms (MOGA)[23]. While more robust than single-objective, multi-objective Genetic algorithms are difficult to implement and computationally expensive [24]. In one successful application of MOGA, Ely, Crossley, and Williams identified a set of constellation design with eccentric orbits, aiming to minimize the orbit altitude and number of satellites [25]. Another multi-objective optimization study varied six orbital elements, 5 of which are optimization design variables, to determine the percent coverage and revisit time as best parameters to analyze the performance of the constellation. This approach was found to be more computationally effective by implementing a semi-analytical approach, and it found a larger population of acceptable solutions [24]. Evolutionary algorithms are another class of MOGA's that aim to reduce computational complexity by controlling the number of iterations that the algorithm explores solutions[26]. Hitomi and Selva found that variable length evolutionary algorithms lead to significantly faster convergence to a higher quality population than fixed length algorithm[27].[28][29] and [30] further proved the effectiveness of evolutionary algorithms for constellation design.

### *2.2. Demand Modeling*

Demand for satellite communications is growing quickly. ITU data has shown consistent growth in overall adoption to the internet, with a 19.1% increase in 2017, and a 17.5% increase in 2018[31]. Total international internet bandwidth has grown more than six fold in less than a decade [31]. In 2018, of the 4,980 satellites in orbit, 775 were used primarily for communications [31]. The overall development of space assets has increased substantially in the past few years, 580 satellites were registered with the United Nations Office for Outer Space Affairs in 2019, and 1264 satelites in 2020 [32].

Satellites offer tremendous reach and can widen access to broadband services. They can broadcast content in a country at a cost that is independent of the number of users. The World Economic Forums's Global Agenda Council on Space Security found that a land-based network cannot support the level of traffic that will come with continually growing demand. [33]. One estimation stated that the internet subscriber growth will level off 11 billion total users in 2050 [34]. Internet users, and those who would like to become internet users, are largely affected by extent, type, reliability, and type of digital infrastructure available both locally, nationally, and globally.

In areas where there is consistent internet coverage, the quality of coverage has been getting faster and faster, leaving unconnected groups behind [35]. As Graydon points out, satellite internet companies often make broad claims about connecting the 'other 3 billion': users that are living in developing regions that are unconnected from the internet. These generalizations often speak for unconnected communities, but there have been few reports analyzing how to effectively bridge unconnected communities to the internet. Graydon's report found that there are fundamental issues regarding unconnected groups surrounding infrastructure, affordability, skills awareness and culture acceptance and local adoption and use [36]. In response to these concerns,this paper will focus on demand in areas where there is no 3-4G coverage, as it is assumed that if terrestrial networks reach those areas, it will always be cheaper than satellite broadband. Constructing fiber optic cables is time consuming and expensive, but still cheaper than the process of developing, launching, and operating a satellite[36].

## 3. Methodology

The methodology followed in this paper is as follows. First, we identify a reduced set of decisions that characterize the most important traits of a satellite constellation, and though the use of a morphological matrix, identify a way to systematically enumerate all constellation designs. Next, we search the design-space of potential architectures looking for the best designs by using tradespace exploration. As opposed to more traditional methods that largely rely on expert opinion and detailed analysis of a few point designs (known as "expert design"), tradespace exploration advocates for the evaluation of a multitude of designs corresponding to different concepts in the design space [37], which yields a better understanding of the trade-offs and relationships between variables in the design-space [38], making this technique suitable for the conceptual design phase.

We identified the following set of decisions that drive the performance and cost for a space-communications constellation: orbital altitude, number of planes, number of satellites per plane, orbital inclination, number of payload beams, as well as the frequencies for the user-satellite links, gateway-satellite links, and inter-satellite links. The design-space is defined as the set of decisions that need to be taken when designing a satellite constellation, together with the options for each decision, an is commonly represented using a morphological matrix as shown in Table 1.

Table 1: Morphological matrix for space systems

Some considerations need to be taken for each of the different decisions:

- **Orbital altitude and inclination**: possible orbital altitudes include GEO (35,768 km), MEO (8,000 km), and LEO (1,200 km). The orbital inclination can take one of the values in $\{0°, 30°, 45°, 60°, 90°\}$, with the following constraints for GEO networks, only equatorial orbits (inclination = 0°) are allowed; for LEO networks, only non-equatorial orbits are allowed.

- **Number of planes and number of satellites per plane**: these decisions determine the overall constellation structure and the total number of satellites. The following constraints apply to the decision: for equatorial configurations (inc=0°), the number of planes is always 1; for non-equatorial configurations, it is always greater than 1. Moreover, for MEO constellations, the maximum number of planes is 20 and the number of satellites per plane is any option

between 5 to 30; finally, only GEO architectures can have 3 satellites per plane, since constellations in other orbits cannot possibly achieve global coverage with such a small number of planes.

- **Number of beams per satellite**: the number of beams per satellite can take any value in {7, 19, 37, 74, 370, 740}. However, the following constraints apply: for LEO networks, the number of beams must be fewer than or equal to 74 beams (due to the assumed power limitations of the spacecraft), whereas GEO networks must have a number of beams greater than or equal to 37 (i.e., architectures comprised of "small- GEO" satellites are not considered). Finally, MEO networks with a large number of planes (10, 20, 50) must have fewer than 100 beams per satellite.

- **Number and locations of ground stations**: although not featured as a decision per-se in the morphological matrix, the number and locations of the ground stations are optimized for each architecture, following the procedure described in Section 3.3.1.

### *3.1. Exploring the search-space*

Based on the number of decisions and options, the total number of potential architectures becomes quite large. Given the large size of the design-space, enumerating all constellation-designs and evaluating them is computationally unfeasible. Therefore, the problem calls for the use of some type of optimization method to select the designs whose performance and economic metrics are to be evaluated.

In this paper we use Bayesian Optimization (BO) based-method to identify the architectures that have the highest potential and will be subject to performance and cost evaluation. BO is a set of optimization techniques used to find the extrema of black-box functions that are expensive to evaluate, and is very effective in minimizing the number of function evaluations required to locate the extrema. Let $f(x)$ be the black-box function which is to be optimized. BO tries to model the unknown function $f(x)$ using a cheaper-to-evaluate model-function $\hat{f}(x)$, and then use $\hat{f}(x)$ to guide the optimization process within the search space by balancing exploration (evaluate new points in unexplored regions) and exploitation (evaluate new points in the proximity of known good solutions). The main idea behind Bayesian optimization is to incorporate prior belief about the space of possible functions $f(x)$ when making the choice of $\hat{f}(x)$. As its name suggests, Bayesian optimization uses *Bayes theorem* to obtain the posterior probability of the model $\hat{f}(x)$ given a set of data observations. In this context, data observations are recorded as the set of pairs $\mathscr{D} = \{(x, f(x))\}_{j=1}^{n}$ that have been evaluated so far. Hence, Bayesian optimization computes a probability distribution for a model-function $\hat{f}(x)$ given the data $\mathscr{D}$ as

$$\Pr(\hat{f}|\mathscr{D}) \propto \Pr(\mathscr{D}|\hat{f})P(\hat{f}) \tag{1}$$

the posterior distribution is used to determine the next evaluation point following some criterion which maximizes the utility of the evaluation. The criterion is commonly given by an *acquisition function* which explicitly captures the balance between exploration and exploitation. Maximizing the acquisition function is much cheaper than evaluating the objective function, and so the computational overhead is reduced. The point resulting from the optimization of the acquisition function is evaluated using the original function $f(x)$, and is then added to the set of observations $\mathscr{D}$, which is used to update the probability distribution of the model $\hat{f}(x)$.

### 3.2. Evaluating one constellation design

The rest of section presents the models used to estimate various aspects of the constellation needed to determine its performance, together with the major assumptions and methodology used to estimate the financial metrics for the constellation.

On one hand, the performance model has three main sub-models: first, a genetic algorithm computes the optimal locations and number of feeder gateways required. Second, an estimate of the demand on each link is created. Finally, the gateway locations and the estimates of the demand are used as inputs for atmosphere models, link budget models, and orbital dynamics models to determine the sellable capability of the constellation through Monte Carlo analysis.

On the other hand, the economic model is also composed of three sub-models: first, the masses of the satellites are estimated using a sizing model. Once the masses have been computed, the resultant number of required launches is calculated along with the associated launch cost. Finally, the total system cost is computed by combining the masses, launch cost, and ground segment design as inputs, the financial model determines the minimum price per Mbps/month required to achieve profitability. Each of the following sections specify the details of each of the sub-models.

### 3.3. Performance model

For each constellation design evaluated, its performance in terms of sellable capacity is determined using a three-step process similar to the one described in [11]. First, the demand is estimated by identifying the areas where underserved and uncovered populations inhabit. Second, the optimal locations and number of feeder gateways required by each constellation are computed using a genetic algorithm. Second, the resulting locations are combined with atmospheric models, link budget models, and orbital dynamic models to determine statistically the total system sellable capacity through Monte Carlo analysis.

#### 3.3.1. Ground Segment Optimization

The optimization is centered around maximizing objective function based on the orbital positions that are covered by the gateway with a throughput of at least 50% of the maximum gateway throughput, under atmospheric conditions present in 5% and 0.5% of the time. It is assumed that minimum elevation angle for ground stations to communicate with a satellite is 10 degrees. Additionally, the optimization seeks to minimize the number of ground stations required. Genetic algorithms are better suited than Bayesian optimization for this specific problem due to the large dimensionality. The added complexity of the geographical structure can speed up the convergence of the optimization algorithm [39].

The optimization itself is divided into 2 phases. In phase A, the optimization considers six regions: Africa, Asia, Europe North America, Oceania, and South America. Then in phase B, the genetic algorithm is applied globally, but uses the best architectures from phase A to generate the initial population. Thus, phase B relies on a good selection from phase A.

#### 3.3.2. Demand Model

To derive realistic estimates of the total system throughput, we developed a demand model that provides an upper bound to the maximum sellable capacity for any satellite at a given orbital position. This was done by fixing the data usage per user and month, and deriving an average throughput per user ($R_b^{(bh)}$)*as* :

$$R_b^{(bh)} = \underbrace{\frac{D_t}{30}}_{data-volume per day} \cdot \overbrace{\frac{B}{24}}^{busy hour ratio} \cdot \underbrace{\frac{1}{60 \cdot 60}}_{conversion to bps} \cdot \overbrace{\frac{(1+\alpha)}{\eta}}^{QoS and utilization ratio} \tag{2}$$

where $D_t$ is the monthly data tonnage (in bits), $B$ is the busy-hour ration (equal to 2.5-3 for backhauling systems), $\alpha$ is a security factor to guarantee a minimum QoS during unexpected peaks (assumed to be equal to 10%), and $\eta$ is the utilization factor (assumed equal to 0.85)..

Depending on the area and level of existing infrastructure, the data tonnage was assumed to be 1GB/month for uncovered persons, 3GB/month for under-served persons, and a 10GB/month for covered persons. The model also analyzes the growth on demand over time, and assumes a conservative compound annual growth rate on the average data-rate per user of 9% over the next 10 years. The demand model intentionally focuses on backhaul infrastructures as used to expand cellphone networks, instead of satisfying the demand of other markets such as end-user, military, inflight, and marine.

For a given orbital altitude (LEO, MEO, GEO) and constellation design (in terms of number of planes and number of satellites), we generated a gridded map (of resolution 0.10.1°in latitude and longitude) that computed the number of uncovered, underserved, and covered people within line of sight of a satellite located in each position of the grid, taking into account the minimum elevation angle constraints imposed by the constellation design. In case that multiple satellites could cover the same region simultaneously, it was assumed that users were evenly distributed across all the satellites within their LoS.

### *3.3.3. Link Budget Model*

The link budget model calculates the throughput of the satellite-to-user and satellite-to-gateway links. The model accounts for the effects of the full RF chain including digital signal modulation to demodulation, power amplification and atmospheric impairments. The link budget engine was designed such that it has the ability to handle both bent-pipe and regenerative architectures, while being designed for fast computation of the optimal MODCOD scheme under different atmospheric conditions.

This study used the atmospheric models provided in the International Telecommunications Union's Recommendation P.618-13, which accounts for tropospheric scintillation, rain impairments, and cloud and fog attenuation. In particular, the python implementation in ITU-Rpy was used [40].

A block-diagram of the link-budget model together with the parameters considered is shown in Fig. 1.

Figure 1: **Link model block diagram**

We first compute the link $C/N_0$ as

$$\frac{C}{N_0} = P_{T_x} - OBO + G_{T_x} + G_{R_x} - L - 10\log_{10}(k\, T_{sys}) \qquad [dB] \tag{3}$$

$$L = FSPL + L_{atm} + L_{RF_{T_x}} + L_{RF_{R_x}} \qquad [dB] \tag{4}$$

where $P_{Tx}$ is the transmitted power (dB), $OBO$ is the power-amplifier output back-off, $G_{T_x}$ and $G_{R_x}$ are the transmitting and receiving antenna gains, respectively (dB), $T_{sys}$ is the system temperature (K), and $L$ is the sum of the losses considered, (dB), which includes the free-space path losses (FSPL), atmospheric losses ($L_{atm}$), and losses in the transmitting and receiving RF chains ($L_{RF_{T_x}}$ and $L_{RF_{R_x}}$).

The system temperature is computed using Friis formula:

$$T_{sys} = T_{ant} \cdot 10^{-(L_{RF}/10)} + T_{atm} \cdot 10^{-(L_{atm}+L_{RF})/10} \qquad [K] \tag{5}$$

where $T_{ant}$ is the antenna temperature (K), $T_{atm}$ is the atmospheric temperature (K), $L_{atm}$ are the total atmospheric losses (dB), and $L_{RF}$ are the RF losses in reception (dB).

Next, the link $E_b/(N+I)$ is computed as

$$\frac{C}{N_0+I} = \left(\frac{1}{CABI} + \frac{1}{CASI} + \frac{1}{CXPI} + \frac{1}{C3IM} + \frac{1}{C/N_0}\right)^{-1} \tag{6}$$

$$\frac{E_b}{N+I} = \frac{C}{N_0+I} \cdot \frac{BW}{R_b} \tag{7}$$

where $R_b$ is the link data rate (see below) (bps) , and $BW$ is the bandwidth allocated to that beam (Hz). Notice how our link budget equation considers four different types of interference (CABI, CASI, CXPI, and C3IM). In Eqs. 6 - 7, all terms are in linear scale. Finally, the beam data rate is computed as

$$R_b = \frac{BW}{1+\alpha_r} \cdot \Gamma\left(\frac{E_b}{N+I}\right) \quad [bps], \tag{8}$$

where $\alpha_r$ is the roll-off factor, and $\Gamma$ is the spectral efficiency of the modulation and coding scheme (MODCOD) (bps/Hz), which in turn is a function of the $E_b/(N+I)$. We assumed that adaptive coding and modulation (ACM) techniques is used, and thus, the MODCOD used on each link is the one that provides the maximum spectral efficiency and satisfies condition

$$\left.\frac{E_b}{N}\right|_{th} \geq \frac{E_b}{N+I} + \gamma \qquad [dB], \tag{9}$$

where $\left.\frac{E_b}{N}\right|_{th}$ is the MODCOD threshold $E_b/(N+I)$ (dB), $\frac{E_b}{N+I}$ is the link energy per bit to noise plus interference ratio (dB) (as described in Eq. 7), and $\gamma$ is the link margin (dB).

### *3.3.4. Total System Throughput Estimation*

Due to the stochastic nature of the system, where the throughput is subject to the varying weather conditions and positions of the satellites, a statistical estimation is used to calculate the

upper bound for maximum sellable capacity. In particular, we use a Monte-Carlo method that considers a set of orbital positions and atmospheric conditions,

To calculate the total system throughput, first the orbits of the satellites on the constellation are propagated for a day. Then, atmospheric attenuation samples for each ground station are modeled. These samples are inputted into the link budget model to determine the achievable link data rates for each of the ground stations. Once the data rates have been calculated, the total system throughput is calculated. The system throughput is dependent on the presence of inter-satellite links, if there are ISLs present, the calculation of total system throughput becomes a little more complex. When ISLs are present, then a subset of 1000 scenarios is calculated to determine the demand captured by the satellite in the case of user ISL, satellite to satellite ISL, and gateway link ISL.

### *3.4. Economic model*

The economic model serves to determine the total cost of the system, its economic feasiblity, and the minimum average selling price (in Mbps/month) that the operator would need to achieve a desired internal rate of return of 15%.

#### *3.4.1. Sizing Model*

To properly assess when the constellation configuration will break even, the model calculates the cost to develop these systems. The satellite sizing model is based off the subsystem model estimation method in [41], which relies on data from communication satellite payloads launched in the last 15 years. Determining the mass of a satellite is an iterative process, and so an initial guess is used to provide a baseline estimate for mass and then the subsystem solves iteratively until the system converges [39].

#### *3.4.2. Launch Cost Model*

Launch cost is computed as the cost per launch vehicle multiplied by the number of launches required. The cost per launch estimation is dependent on a historical backlog of operational and developmental launch vehicles, as well as their associated cost and fairing size. To validate the feasibility of the satellite sizing, a constraint is imposed that the satellites must fit within the fairing volume. Then the number of satellites per launch vehicle is scaled accordingly until the all constellation satellites are manifested on a vehicle [39]. From there, the cost to launch all the satellites is determined.

#### *3.4.3. Financial Model*

The financial model calculates the minimum average price per Mbps/month that the company must charge to achieve a 15% iterative rate of return (IRR). The economic feasibility of the constellation takes into account the revenue, CapEx, and the operational expenditure (OpEx) items. CapEx is comprised of the satellite manufacturing costs, launch costs, insurance costs, ground segment costs, and RD costs. OpEx is comprised of ground segment sustainment costs, back-haul costs, and other operational expenses. Cash flow projections are computed assuming a 20-year horizon, with the satellites first launched in year 2, and service operations in year 3. Capacity is sold progressively, and the average price per Mbps/month is chosen so that IRR within a 20-year horizon is 15% [39]. Progress fill factors have not been included.

## 4. Model Validation

The models described in the previous section were validated by comparing the total system throughput predicted against current systems. Table 2 demonstrates the error between the total system throughput of existing systems, and the models estimation. This model consistently underestimates the sellable throughput of Viasat-1 and Viasat-3 by approximately 13%; whereas for OneWeb, the predicted figure is within the range of the reported values. A possible reason for the lower values of Viasat's satellites is that the model estimates sellable throughput with the statistics for atmospheric attenuation taken into account, whereas values reported by the satellite operators are typically under clear-sky conditions. Given the low relative errors, the model is sufficient for the analysis carried out in this paper.

Table 2: Validation of the performance model

For the satellite sizing model, the work was validated by comparing the estimates with historical missions. The satellite-sizing model validation is conducted by comparing the estimates produced by the model against actual values from the TelAstra 2016 database, which contains more than 100 records of past communications missions (both in LEO and GEO). The records in the database date back to as early as 1972 (ANIK A), while the latest record being from 2016 (Viasat-1).

Table 3: Comparison of predicted and actual values for the subsystem and satellite masses for 5 LEO satellites

Table 3 presents the actual values along with the relative errors of the model. For the five spacecraft considered, it is assumed that the payload mass was provided as an input to the sizing algorithm. It can be observed that the predicted launch mass is within 15% of the actual launch mass for all satellites, whereas the predicted satellite dry mass is within 8% of actual values for all cases but Iridium (for which our model overestimates the mass of the structure subsystem). In terms of relative errors by subsystem, the TTC subsystem shows the largest deviations; however, since its mass is relatively small compared to the total mass of the spacecraft, it has a small impact on the final values for the dry and launch masses.

To validate the satellite-sizing model for GEO satellites, six different communications missions were selected (from both commercial and governmental organizations). These missions include Arabsat, TDRSS-J, Telstar-4, Viasat-1, Wildblue, and Koreasat, whose masses range from 1,000 kg (characteristic of missions from small operators) to more than 6 tonnes (characteristic of latest generation HTS launched by well-established operators). Table 4 presents the actual masses along with model errors. Again, it is assumed that the payload mass for each of the satellites was provided as an input to the algorithm. The results obtained for GEO satellites are similar to those obtained for LEO satellites; the launch-mass errors are within 10% error for all satellites but TDRSS-J, whereas the dry-mass errors are within 17% in all cases.

Given the results from the validation process, it can be concluded that the satellite sizing model is accurate enough for tradespace exploration in the context of space communications constella-

Table 4: Comparison of predicted and actual values for the subsystem and satellite masses for 6 GEO satellites

tions. Moreover, the effects that the uncertainty (or errors) of the satellites-sizing model have on the output metric will be further studied through sensitivity analysis.

Similarly, for the cost model, this work was validated by comparing the cost estimates against several legacy systems. The model estimates correspond to the sum for the non-recurring and recurring costs of each unit. For constellations where more than one unit was produced, the non-recurring costs are uniformly allocated to each of the satellites, whereas the recurring costs are the average recurring costs after taking into account all discounts associated with the learning rate (i.e., discounts from mass-manufacturing).

Table 5 reports the cost values estimates for the 6 GEO satellites, whereas Table 6 contains the estimate values for the 5 LEO satellites. All cost values (both estimates and actual values) are quoted in the year each satellite was manufactured.

Table 5: Comparison of model and actual cost for 6 GEO satellites

Table 6: Comparison of model and actual cost for 5 LEO satellites

It can be observed that the cost model does provide reasonable estimates for both LEO and GEO satellites. Overall, relative cost errors are within 30% of the real values. Although these errors might seem high at first glance, it is not uncommon for cost models to deviate by such magnitudes (in fact, a 30% error would be considered relatively modest in terms of cost estimation). Importantly, these cost estimates only need to be accurate enough to allow for comparison among architectures in the tradespace exploration.

## 5. Results and Discussion

In this section, we show the tradespace exploration results for space networks. We investigate the effect of constellation sellable capacity on price per Mbps/month across GEO, MEO, and LEO designs. Figure 2 shows the tradespace exploration results. Each point corresponds to a constellation, that is, a unique combination of decision-options from Table 1. The horizontal axis represents the capital expenditure required to begin operations, whereas the vertical axis is the total sellable forward link (FWD) capacity. In addition to the constellation designs obtained from the morphological matrix, values for several of the currently-proposed systems have been included in the graph. The yellow dot at the top-left corner represents the utopia point, that is, the ideal (unattainable) point (where infinite capacity is available at close-to-zero capital expenditure costs).

Figure 2: Tradespace exploration results for satellite networks. Each point represents a different constellation design. The yellow dot at the upper left corner is the utopia point (ideal value).

Figure 2 lacks two elements that are required to understand the tradespace fully: first, the operational expenditure and replenishment costs are not taken into account, and second, the throughput offered by the different architectures relative to demand (i.e., whether the architectures are over-provisioning or under-provisioning capacity), which in turn is a function of the price.

Figure 3: Demand curve and tradespace exploration results for satellite networks. Each point represents a different architecture. The black curve represents the global broadband demand as a function of the price

Figure 3 shows an alternative view of the tradespace, in which the horizontal axis represents the minimum cost per Mbps/month that each architecture would need to sell its capacity to achieve 15% IRR. 15% IRR was selected after discussions with industry investors. The black line represents the estimated demand for the broadband market, hence, architectures over the black line can be interpreted as over-provisioning capacity (and thus will not be able to sell all their capacity at the targeted price), whereas those below the line are under-provisioning. Note that the demand curve represents the "global" broadband + backhaul market demand curve.

From figure 3, only a small proportion of architectures are viable businesses. Of the businesses shown on the graph above the line, they may have to raise prices, or target markets that are more profitable than consumer. The bottom left of the graph is the utopia point, which means architectures closer to there have a higher likelihood of being profitable. In that sense, GEO and MEO architecture present the highest likelihoods of profitability, but LEO systems may be competitive if designed wisely. Another important point is that if all the currently-proposed satellite systems were to be launched (with their designs unchanged), there will be an overall excess of capacity. In particular, total capacity would be more than 40 Tbps of capacity, an amount over 20 times higher than the current global communication satellite capacity.

We mentioned that GEO, MEO, and LEO designs can all be competitive if they are designed wisely. In particular, tables 7, 8, and 9 show the most popular options for the decisions among architectures that indicate the highest likelihoods of being profitable (i.e., those farthest to the bottom-left of the demand curve in the above figure). This analysis was done under the assumption that the market capture was fixed, and independent of the number of players. For each table, the morphological matrix of decisions is depicted, and the different options are colored based on their popularity among Pareto-optimal architectures. The more intense the coloring, the more popular an option is.

Table 7: Popularity of decision-options for GEO architectures on the Pareto front. The color intensity is proportional to the number of times each option was present in Pareto optimal architectures.

Table 8: Popularity of decision-options for MEO architectures on the Pareto front. The color intensity is proportional to the number of times each option was present in Pareto optimal architectures.

Table 9: Popularity of decision-options for LEO architectures on the Pareto front. The color intensity is proportional to the number of times each option was present in Pareto optimal architectures.

From figure 4, it can be observed that MEO and GEO networks would be able to offer lower prices per Mbps/month than LEO networks and still be profitable, which are, on average, 27% times more expensive. As for the number of planes and the number of satellites per plane, the smaller the number of planes and of satellites per plane, the lower the price per Mbps/month. This

merely confirms that there are diminishing returns for large constellations, as most of the value is delivered by the initial satellites. It is also interesting to note that the higher the number of beams per satellite, the lower the cost per Mbps/month. This supports the hypothesis that it is more cost-effective to have a small number of highly-capable satellites (similar to the current vHTS proposals in GEO and MEO) than many low-complexity satellites (as in current LEO megaconstellations proposals by SpaceX, OneWeb, and Telesat). Finally, with regard to the frequency of operation, there is a reduction of 8% in the price per Mbps/month when transitioning feeder links into higher frequency-bands (i.e., moving from Ka-band to Q/V or E band), and a similar effect is observed for the user frequency, where the Q-band offers the lowest price per Mbps/month. Finally, E-band ISLs result in a 10% increase in the price per Mbps/month, whereas using the optical band allows for a reduction of 5%.

Figure 4: Main effect of decision for satellite networks on price per Mbps/month. Each subplot corresponds to a different decision. The patches represent the 95% confidence interval for the main effect and were computed by bootstrapping (10,000 replicas)

Figure 5: Main effect of decision for satellite networks on sellable capacity. Each subplot corresponds to a different decision. The patches represent the 95% confidence interval for the main effect and were computed by bootstrapping.

Figure 5 shows the main effect on the sellable capacity of the main satellite network decisions. Out of all decisions, the ISL frequency and user frequency play the least important roles and are not significant when computing the sellable capacity of a network. The type of orbit has a large impact, with MEO networks providing on average 25% more throughput than LEO networks. This is mainly a consequence of the design constraints imposed on such networks (it would not make sense to have a LEO network composed of 6 tonnes vHTS). As expected, other decisions such as the number of beams, the number of planes, and the number of satellites per plane, all have a strong effect on the sellable capacity: the more beams/planes/satellites,the higher the network's sellable capacity. Finally, in terms of orbit inclination, polar orbits (90°) result in 60% less sellable capacity, whereas inclinations of 30°and 45°result in moderate gains of around 20%.

## 6. Conclusion

Our analysis concludes that GEO and MEO satellite constellations are the most affordable and viable space architectures to extend connectivity to uncovered and under-served regions. For GEO networks, the dominant architectures have a small number of satellites (3-10) carrying highly-capable payloads (>1 Tbps of throughput), and use higher frequency bands for user and feeder links. For MEO satellites, a larger number of moderate-capacity spacecraft in an equatorial orbit is preferred. Finally, some LEO constellations can also be competitive; the model predicts that the best designs would feature a relatively small number of satellites (200-450) with simple payloads, no crosslinks, and positioned at inclined orbits.

It is envisioned that the next generation of satellites (to be launched within the next 2-5 years) will bring down prices to $100/Mbps/month, which represents an estimated demand of 5 Tbps

(currently the global satellite capacity for data networks is below 2 Tbps). Given these prices, our demand model estimates that satellite systems will be affordable for up to 120 million currently uncovered and under-served people worldwide. However, further reductions in price may be achievable for the future generations of satellites (8-10 years); if prices drop below the $35/Mbps/month threshold, the number of additional people currently uncovered and under-served for whom satellite backhaul could be affordable would rise to 300 million worldwide.

There are two important technology trends that could allow for lower costs per capacity unit for future satellite systems. First, transitioning to higher frequency bands (for both the user and feeder links) will enable cost reductions by increasing the sellable capacity. Second, further miniaturization and integration of components will enable payload weights to be further reduced, which in turn could enable lower satellite costs.

## 7. Acknowledgements

The authors would like to thank Facebook and the Fundacion Obra Social de La Caixa for partially funding this project. The content of this article does not reflect the official opinions of these organizations. Responsibility for the information and views expressed herein lies entirely with the authors

## References

[1] E. W. Ashford, Non-geo systems—where have all the satellites gone?, Acta Astronautica 55 (3-9) (2004) 649–657. doi:10.1016/j.actaastro.2004.05.018.

[2] R. Fildes, V. Kumar, Telecommunications demand forecasting—a review, International Journal of Forecasting 18 (4) (2002) 489–522. doi:10.1016/s0169-2070(02)00064-x.

[3] J. W. Mayo, O. Ukhaneva, International telecommunications demand, Information Economics and Policy 39 (2017) 26–35. doi:10.1016/j.infoecopol.2017.02.001.

[4] A. Mann, Starlink: Spacex's satellite internet project (Jan 2020).
URL https://www.space.com/spacex-starlink-satellites.html

[5] Fcc grants oneweb access to us market for its proposed new broadband satellite constellation, Federal Communications Commission.
URL https://www.fcc.gov/document/fcc-grants-oneweb-us-access-broadband-satellite-constellation

[6] F. C. Commission, Fcc fact sheet viasat authorization, URL: https://docs.fcc.gov/public/attachments/DOC-363487A1.pdf (Apr 2020).

[7] Connect 2020 agenda, URL: https://www.itu.int/en/ITU-D/LDCs/Pages/Connect-2020-Agenda.aspx.

[8] U. B. Commission, 2025 targets: "connecting the other half".
URL https://broadbandcommission.org/Documents/publications/wef2018.pdf

[9] R. Thanki, Measuring the local impact of tvws broadband, URL: http://dynamicspectrumalliance.org/assets/DSA_Presentations/5-1_DSA_2015_GlobalSummit_Day2_Richard_Thanki.pdf (2015).

[10] I. Philbeck, Connecting the unconnected: Working together to achieve connect 2020 agenda targets.

[11] I. D. Portillo, B. G. Cameron, E. F. Crawley, A technical comparison of three low earth orbit satellite constellation systems to provide global broadband, Acta Astronautica 159 (2019) 123–135. doi:10.1016/j.actaastro.2019.03.040.

[12] M. Wittig, A highly innovative global broadband mobile communication system concept, Acta Astronautica 66 (7-8) (2010) 1113–1124. doi:10.1016/j.actaastro.2009.09.032.

[13] L. A. Singh, W. R. Whittecar, M. D. Diprinzio, J. D. Herman, M. P. Ferringer, P. M. Reed, Low cost satellite constellations for nearly continuous global coverage, Nature Communications 11 (1). doi:10.1038/s41467-019-13865-0.

[14] T. G. Reid, A. M. Neish, T. Walter, P. K. Enge, Broadband leo constellations for navigation, Navigation 65 (2) (2018) 205–220. doi:10.1002/navi.234.

[15] Iridium: failures successes, Acta Astronautica 48 (2001) 817–825. doi:10.1016/S0094-5765(01)00036-4.

[16] A. G. Alkholidi, K. S. Altowij, Free space optical communications — theory and practices, Contemporary Issues in Wireless Communicationsdoi:10.5772/58884.

[17] Y. Fujiwara, M. Mokuno, T. Jono, T. Yamawaki, K. Arai, M. Toyoshima, H. Kunimori, Z. Sodnik, A. Bird, B. Demelenne, et al., Optical inter-orbit communication engineering test satellite (oicets), 57th International Astronautical Congressdoi:10.2514/6.iac-06-b3.5.10.

[18] J. A. Kéchichian, Analysis and implementation of in-plane stationkeeping of continuously perturbed walker constellations, Acta Astronautica 65 (11-12) (2009) 1650–1667. doi:10.1016/j.actaastro.2009.04.008.

[19] E. Lansard, E. Frayssinhes, J.-L. Palmade, Global design of satellite constellations: a multi-criteria performance comparison of classical walker patterns and new design patterns, Acta Astronautica 42 (9) (1998) 555–564. doi:10.1016/s0094-5765(98)00043-5.

[20] The art of satellite constellation design: What you need to know (Jul 2015). URL https://www.astrome.co/blogs/the-art-of-satellite-constellation-design-what-you-need-to-know/

[21] C. Han, S. Bai, S. Zhang, X. Wang, X. Wang, Visibility optimization of satellite constellations using a hybrid method, Acta Astronautica 163 (2019) 250–263. doi:10.1016/j.actaastro.2019.01.025.

[22] W. A. Crossley, E. A. Williams, Simulated annealing and genetic algorithm approaches for discontinuous coverage satellite constellation design, Engineering Optimization 32 (3) (2000) 353–371. doi:10.1080/03052150008941304.

[23] T. Murata, H. Ishibuchi, H. Tanaka, Multi-objective genetic algorithm and its applications to flowshop scheduling, Computers  Industrial Engineering 30 (4) (1996) 957–968. doi:10.1016/0360-8352(96)00045-9.

[24] T. Savitri, Y. Kim, S. Jo, H. Bang, Satellite constellation orbit design optimization with combined genetic algorithm and semianalytical approach, International Journal of Aerospace Engineering 2017 (2017) 1–17. doi:10.1155/2017/1235692.

[25] T. A. Ely, W. A. Crossley, E. A. Williams, Satellite constellation design for zonal coverage using genetic algorithms, AAS/AIAA Space Flight Mechanics Meeting (1998) 98–128.

[26] C. A. Coello Coello, An introduction to evolutionary algorithms and their applications, in: F. F. Ramos, V. Larios Rosillo, H. Unger (Eds.), Advanced Distributed Systems, Springer Berlin Heidelberg, Berlin, Heidelberg, 2005, pp. 425–442.

[27] N. Hitomi, D. Selva, Constellation optimization using an evolutionary algorithm with a variable-length chromosome, 2018 IEEE Aerospace Conferencedoi:10.1109/aero.2018.8396743.

[28] X. Wang, H. Zhang, S. Bai, Y. Yue, Design of agile satellite constellation based on hybrid-resampling particle swarm optimization method, Acta Astronautica 178 (2021) 595–605. doi:10.1016/j.actaastro.2020.09.040.

[29] J. R. Gagliano, Orbital constellation design and analysis using spherical trigonometry and genetic algorithms: A mission level design tool for single point coverage on any planetdoi:10.15368/theses.2018.100.

[30] W. R. Whittecar, M. P. Ferringer, Global coverage constellation design exploration using evolutionary algorithms, AIAA/AAS Astrodynamics Specialist Conferencedoi:10.2514/6.2014-4159.

[31] The state of broadband 2019 report highlights.
URL https://broadbandcommission.org/Documents/SOBB-REPORTHIGHTLIGHTS-v3.pdf

[32] Online index of objects launched into outer space (Feb 2021).
URL https://www.unoosa.org/oosa/osoindex/search-ng.jspx?lf_id=

[33] Bringing Space Down to Earth, 2015.
URL http://www3.weforum.org/docs/WEF_Bringing_Space_Down_to_Earth.pdf

[34] M. Wittig, Internet access for everybody: The satellite solution, Acta Astronautica 64 (2-3) (2009) 222–229. doi:10.1016/j.actaastro.2008.07.012.

[35] L. Philip, C. Cottrill, J. Farrington, F. Williams, F. Ashmore, The digital divide: Patterns, policy and scenarios for connecting the 'final few' in rural communities across great britain, Journal of Rural Studies 54 (2017) 386–398. doi:10.1016/j.jrurstud.2016.12.002.

[36] M. Graydon, L. Parks, 'connecting the unconnected': a critical assessment of us satellite internet services, Media, Culture Society 42 (2) (2019) 260–276. doi:10.1177/0163443719861835.

[37] A. M. Ross, D. E. Hastings, 11.4.3 the tradespace exploration paradigm, INCOSE International Symposium 15 (1) (2005) 1706–1718. doi:10.1002/j.2334-5837.2005.tb00783.x.

[38] M. E. Fitzgerald, A. M. Ross, Controlling for framing effects in multi-stakeholder tradespace exploration, Procedia Computer Science 28 (2014) 412–421. doi:10.1016/j.procs.2014.03.051.

[39] I. Portillo, Space and aerial architectures to expand global connectivity, Ph.D. thesis (2020). URL http://systemarchitect.mit.edu/docs/delportillo19b.pdf

[40] ITU, Propagation data and prediction methods required for the design of earth-space telecommunication systems, Recommendation ITU-R (2015) 618–621.

[41] J. R. Wertz, D. F. Everett, J. J. Puschell, Space mission engineering: the new SMAD, Microcosm Press, 2011.

## 8. Author's Biographies

**Iñigo del Portillo** works for SES, a global satellite operator, as Systems Engineer. He received his BS degrees in Telecommunications Engineering, and Industrial Engineering in 2014, and a MSc in electronics engineering in 2015, all of them from Universitat Politecnica de Catalunya in Barcelona, Spain. In 2016 he obtained a MSc. degree in Aeronautics and Astronautics from MIT, and in 2019 he completed his Ph.D. at MIT. His interests include space and aerial communication networks to extend broadband availability worldwide, optical communications for space based networks, and small satellite communications. He has previously worked at Facebook, GKN LandSystems and at Procter Gamble.

**Sydney Dolan** is a third year graduate student and NSF Fellow in MIT's Aeronautics and Astronautics Department. Prior to MIT, she received her B.S. in Aerospace Engineering from Purdue University. Previously, she has worked at a wide range of companies within commercial space including NanoRacks, Blue Origin, Aerospace Corporation, and Advanced Space. Her research interests are at the cross-section of space systems and artificial intelligence, where she wants to create provably safe, verifiable machine learning algorithms for flight hardware.

**Bruce G. Cameron** is the Director of the System Architecture Group at MIT. His research interests include technology strategy, system architecture, and the management of product platforms. Additionally, Dr. Cameron is the Faculty Director for MIT's Architecture and System Engineering online certificate, which has taught over 9500 participants. Previously, Dr. Cameron worked in high tech and banking, where he built advanced analytics for managing complex development programs.

**Edward F. Crawley** received an Sc.D. in Aerospace Structures from MIT in 1981. His early research interests centered on structural dynamics, aeroelasticity, and the development of actively controlled and intelligent structures. Recently, Dr. Crawley's research has focused on the domain of the architecture and design of complex systems.

Dr. Crawley is a Fellow of the AIAA and the Royal Aeronautical Society (UK), and is a member of three national academies of engineering: the Royal Swedish Academy of Engineering Science, the (UK) Royal Academy of Engineering, and the US National Academy of Engineering. He is the author of numerous journal publications in the AIAA Journal, the ASME Journal, the Journal of Composite Materials, and Acta Astronautica.

## 9. Figures and Tables

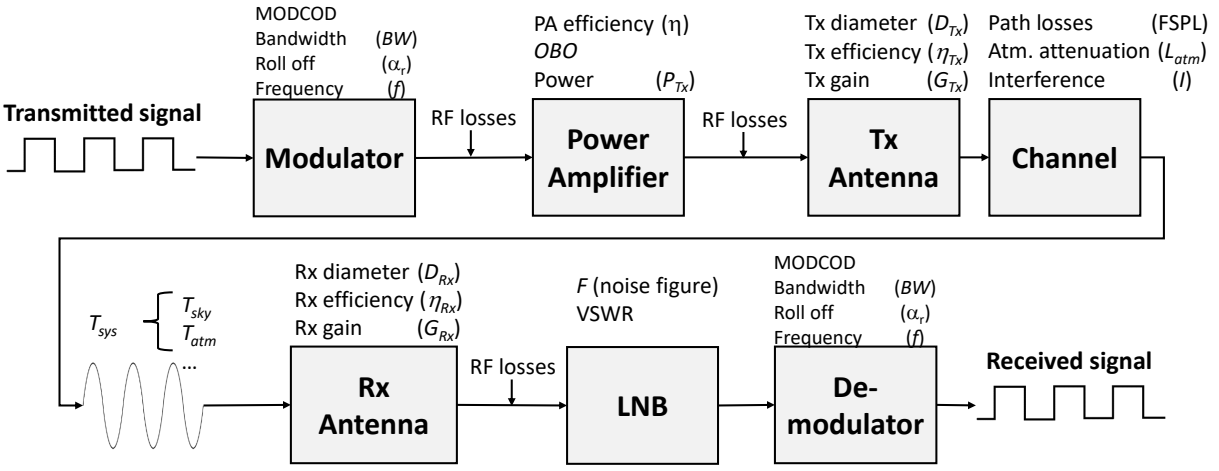


Figure 1:**Link model block diagram**

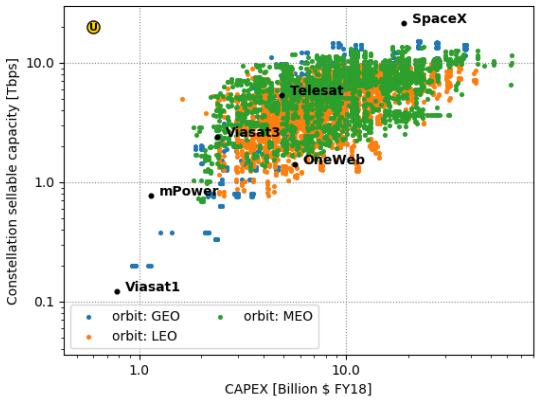


Figure 2: Tradespace exploration results for satellite networks. Each point represents a different constellation design. The yellow dot at the upper left corner is the utopia point (ideal value).

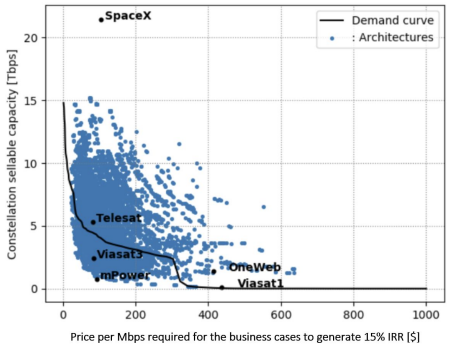


Figure 3: Demand curve and tradespace exploration results for satellite networks. Each point represents a different architecture. The black curve represents the global broadband demand as a function of the price

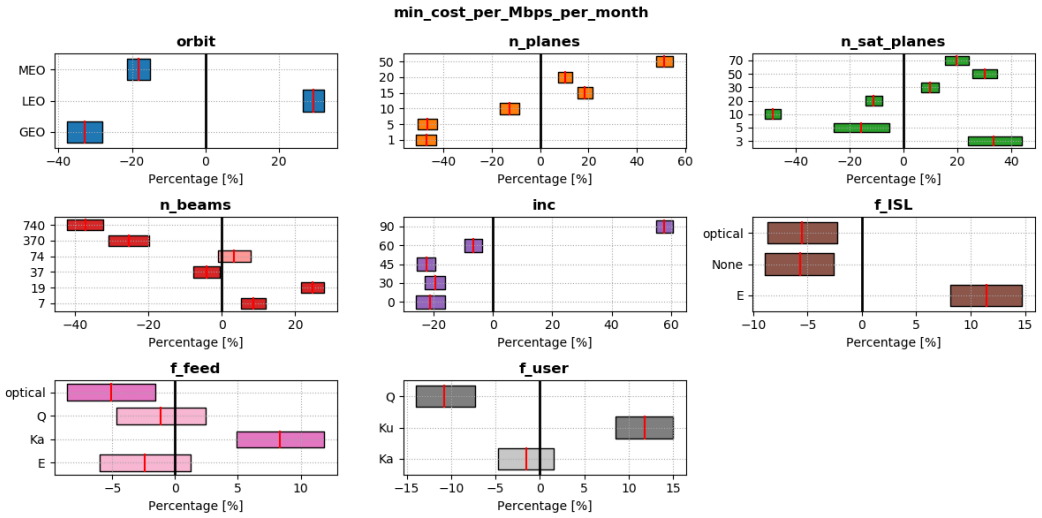


Figure 4: Main effect of decision for satellite networks on price per Mbps/month. Each subplot corresponds to a different decision. The patches represent the 95% confidence interval for the main effect and were computed by bootstrapping (10,000 replicas)

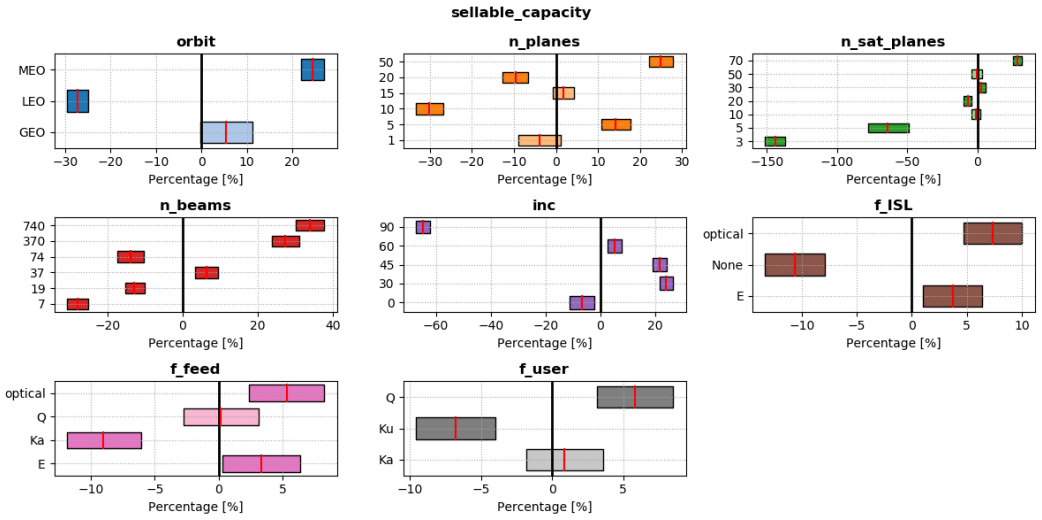


Figure 5: Main effect of decision for satellite networks on sellable capacity. Each subplot corresponds to a different decision. The patches represent the 95% confidence interval for the main effect and were computed by bootstrapping.

Table 1: Morphological matrix for space systems

| Decision name | Decision options | | | | | | |
|---|---|---|---|---|---|---|---|
| **Orbital Altitude** | GEO | MEO | LEO | | | | |
| **Number of planes** | 1 | 5 | 10 | 15 | 20 | 50 | |
| **Number of satellites / plane** | 3 | 5 | 10 | 20 | 30 | 50 | 70 |
| **Orbital inclination** | 0 | 30 | 45 | 60 | 90 | | |
| **Number of payload beams** | 7 | 19 | 37 | 74 | 370 | 740 | |
| **Frequency User $\leftrightarrow$ Satellite** | Ku | Ka | V/Q | | | | |
| **Frequency Satellite $\leftrightarrow$ Gateway** | Ka | V/Q | E | Optical | | | |
| **Frequency Inter-satellite Links** | E | Optical | None | | | | |

Table 2: Validation of the performance model

| | Sellable capacity [Gbps] | | |
|---|---|---|---|
| **System** | **Model** | **Truth** | **Error (%)** |
| **Viasat-1** | 122.3 | 140 | -12.8 % |
| **Viasat-3** | 865 | 1,000 | -13.5 % |
| **OneWeb** | 1,506 | 1,400 | 7.57 % |

Table 3: Comparison of predicted and actual values for the subsystem and satellite masses for 5 LEO satellites

| Satellite | Globalstar | | | Iridium | | | Teledesic | | |
|---|---|---|---|---|---|---|---|---|---|
| | Model | Actual | % error | Model | Actual | % error | Model | Actual | % error |
| Payload | 115.0 | 115.0 | 0.0 | 338.5 | 338.5 | 0.0 | 283.4 | 283.4 | 0.0 |
| Structure | 68.4 | 60.0 | 14.0 | 157.0 | 51.0 | 207.9 | 268.0 | 273.5 | -2.0 |
| Telecommand | 11.2 | 1.0 | 1021.5 | 25.8 | - | - | 44.0 | 17.7 | 148.4 |
| EPS | 117.4 | 104.0 | 12.9 | 215.1 | 161.7 | 33.0 | 665.9 | 513.6 | 29.6 |
| ADCS | 17.4 | 32.0 | -45.5 | 23.2 | 20.1 | 15.5 | 30.1 | 23.6 | 27.5 |
| Thermal | 9.6 | 23.0 | -58.4 | 22.0 | 24.8 | -11.4 | 37.5 | 72.8 | -48.5 |
| Dry-mass | 341.9 | 350.0 | -2.3 | 785.1 | 613.7 | 27.9 | 1340.3 | 1350.0 | -0.7 |
| Launch-mass | 406.3 | 410.0 | -0.9 | 884.0 | 780.0 | 13.3 | 1592.8 | 1490.0 | 6.9 |

| Satellite | Skybridge | | | Globalstr2 | | |
|---|---|---|---|---|---|---|
| | Model | Actual | % error | Model | Actual | % error |
| Payload | 400.0 | 400.0 | 0.0 | 300.0 | 300.0 | 0.0 |
| Structure | 247.3 | - | - | 145.4 | - | - |
| Telecommand | 40.6 | - | - | 23.8 | - | - |
| EPS | 474.4 | - | - | 208.5 | - | - |
| ADCS | 28.8 | - | - | 22.5 | - | - |
| Thermal | 34.6 | - | - | 20.4 | - | - |
| Dry-mass | 1236.7 | 1250.0 | -1.1 | 726.8 | 676.0 | 7.5 |
| Launch-mass | 1476.4 | 1538.0 | -4.0 | 864.7 | 832.0 | 3.9 |

Table 4: Comparison of predicted and actual values for the subsystem and satellite masses for 6 GEO satellites

| Satellite | Arabsat | | | TDRSS-J | | | Telstar-4 | | |
|---|---|---|---|---|---|---|---|---|---|
| | Model | Actual | % error | Model | Actual | % error | Model | Actual | % error |
| Payload | 122.4 | 122.4 | 0.0 | 625.0 | 625.0 | 0.0 | 390.7 | 390.7 | 0.0 |
| Structure | 104.5 | 90.4 | 15.6 | 280.1 | 305.5 | -8.3 | 316.5 | 176.4 | 79.4 |
| Telecommand | 17.1 | 29.2 | -41.3 | 45.9 | 52.1 | -11.8 | 51.9 | 78.5 | -33.9 |
| EPS | 182.6 | 177.0 | 3.1 | 268.6 | 434.0 | -38.1 | 625.1 | 566.7 | 10.3 |
| ADCS | 56.0 | 66.5 | -15.9 | 74.4 | 138.9 | -46.4 | 77.9 | 70.6 | 10.4 |
| Thermal | 14.6 | 30.2 | -51.6 | 39.2 | 76.4 | -48.7 | 44.3 | 90.7 | -51.1 |
| Dry-mass | 522.3 | 573.1 | -8.9 | 1400.6 | 1736.0 | -19.3 | 1582.6 | 1621.0 | -2.4 |
| Launch-mass | 990.4 | 1140.0 | -13.1 | 2655.9 | 3196.0 | -16.9 | 3000.9 | 3331.2 | -9.9 |

| Satellite | Viasat-1 | | | Wildblue | | | Koreasat-1 | | |
|---|---|---|---|---|---|---|---|---|---|
| | Model | Actual | % error | Model | Actual | % error | Model | Actual | % error |
| Payload | 794.1 | 794.1 | 0.0 | 500.0 | 500.0 | 0.0 | 202.0 | 202.0 | 0.0 |
| Structure | 698.5 | 532.3 | 31.2 | 416.5 | - | - | 127.6 | - | - |
| Telecommand | 114.6 | 159.8 | -28.3 | 68.3 | - | - | 20.9 | - | - |
| EPS | 1507.7 | 824.0 | 83.0 | 851.9 | - | - | 180.1 | - | - |
| ADCS | 112.0 | 155.7 | -28.0 | 87.3 | - | - | 58.6 | - | - |
| Thermal | 97.8 | 313.9 | -68.8 | 58.3 | - | - | 17.9 | - | - |
| Dry-mass | 3492.8 | 3296.6 | 6.0 | 2082.5 | 1925.0 | 8.2 | 637.8 | 641.0 | -0.5 |
| Launch-mass | 6623.2 | 6739.6 | -1.7 | 3948.8 | 4451.0 | -11.3 | 1209.4 | 1411.0 | -14.3 |

Table 5: Comparison of model and actual cost for 6 GEO satellites

| Name | Actual [$M] | # sats - | Model Est | Model % error |
|---|---|---|---|---|
| Arabsat | 45.0 | 3.0 | 38.2 | -15.1 |
| TDRSS-J | 229.0 | 1.0 | 233.2 | 1.8 |
| Telstar-4 | 70.0 | 3.0 | 93.3 | 33.3 |
| Viasat-1 | 501.0 | 1.0 | 556.7 | 11.1 |
| Wildblue | 265.0 | 1.0 | 286.7 | 8.2 |
| Koreasat-1 | 78.0 | 2.0 | 71.3 | -8.5 |

Table 6: Comparison of model and actual cost for 5 LEO satellites

| Name | Actual [$M] | # sats - | Model Est | Model % error |
|---|---|---|---|---|
| Globalstar | 12.0 | 56.0 | 10.9 | -9.1 |
| Iridium | 24.0 | 66.0 | 19.7 | -18.1 |
| Teledesic | 35.0 | 324.0 | 30.2 | -13.8 |
| Skybridge | 36.0 | 80.0 | 37.5 | 4.2 |
| Globalstr2 | 22.0 | 48.0 | 28.8 | 30.8 |

Table 7: Popularity of decision-options for GEO architectures on the Pareto front. Popularity of decision-options for GEO architectures on the Pareto front. The color intensity is proportional to the number of times each option was present in Pareto optimal architectures.

| **Decision name** | **Decision Options** | | | | | | |
|---|---|---|---|---|---|---|---|
| **Number of planes** | 1 | 5 | 10 | 15 | 20 | 50 | |
| **Number of satellites / plane** | 3 | 5 | 10 | 20 | 30 | 50 | 70 |
| **Orbital inclination** | 0 | 30 | 45 | 60 | 90 | | |
| **Number of payload beams** | 7 | 19 | 37 | 74 | 370 | 740 | |
| **Frequency User ↔ Satellite** | Ku | Ka | V/Q | | | | |
| **Frequency Satellite ↔ Gateway** | Ka | V/Q | E | Optical | | | |
| **Frequency Inter-satellite Links** | None | E | Optical | | | | |

Table 8: Popularity of decision-options for MEO architectures on the Pareto front. Popularity of decision-options for MEO architectures on the Pareto front. The color intensity is proportional to the number of times each option was present in Pareto optimal architectures.

| **Decision name** | **Decision Options** | | | | | | |
|---|---|---|---|---|---|---|---|
| **Number of planes** | 1 | 5 | 10 | 15 | 20 | 50 | |
| **Number of satellites / plane** | 3 | 5 | 10 | 20 | 30 | 50 | 70 |
| **Orbital inclination** | 0 | 30 | 45 | 60 | 90 | | |
| **Number of payload beams** | 7 | 19 | 37 | 74 | 370 | 740 | |
| **Frequency User ↔ Satellite** | Ku | Ka | V/Q | | | | |
| **Frequency Satellite ↔ Gateway** | Ka | V/Q | E | Optical | | | |
| **Frequency Inter-satellite Links** | None | E | Optical | | | | |

Table 9: Popularity of decision-options for LEO architectures on the Pareto front. Popularity of decision-options for LEO architectures on the Pareto front. The color intensity is proportional to the number of times each option was present in Pareto optimal architectures.

| Decision name | Decision Options | | | | | | |
|---|---|---|---|---|---|---|---|
| **Number of planes** | 1 | 5 | 10 | 15 | 20 | 50 | |
| **Number of satellites / plane** | 3 | 5 | 10 | 20 | 30 | 50 | 70 |
| **Orbital inclination** | 0 | 30 | 45 | 60 | 90 | | |
| **Number of payload beams** | 7 | 19 | 37 | 74 | 370 | 740 | |
| **Frequency User $\leftrightarrow$ Satellite** | Ku | Ka | V/Q | | | | |
| **Frequency Satellite $\leftrightarrow$ Gateway** | Ka | V/Q | E | Optical | | | |
| **Frequency Inter-satellite Links** | None | E | Optical | | | | |